

Temozolomide induces senescence and repression of DNA repair pathways in glioblastoma cells via activation of ATR-CHK1, p21, and NF- κ B

Dorthe Aasland, Laura Götzinger, Laura Hauck, Nancy Berte, Jessica Meyer, Melanie Effenberger, Simon Schneider, Emelie E. Reuber, Wynand P. Roos, Maja T. Tomicic*, Bernd Kaina* and Markus Christmann*

Department of Toxicology, University Medical Center Mainz, Obere Zahlbacher Str. 67,
D-55131 Mainz, Germany

*Corresponding authors:

Markus Christmann: mchristm@uni-mainz.de, 0049-6131-179066, Obere Zahlbacher Str. 67,
D-55131 Mainz, Germany, Department of Toxicology, University Medical Center Mainz

Bernd Kaina: kaina@uni-mainz.de, 0049-6131-179217, Obere Zahlbacher Str. 67, D-55131
Mainz, Germany, Department of Toxicology, University Medical Center Mainz

Maja T. Tomicic: tomicic@uni-mainz.de, 0049-6131-179257, Obere Zahlbacher Str. 67, D-
55131 Mainz, Germany, Department of Toxicology, University Medical Center Mainz

Summary

The DNA methylating drug temozolomide (TMZ), which induces cell death through apoptosis, is used for the treatment of malignant glioma. Here we investigate the mechanisms underlying the ability of TMZ to induce senescence in glioblastoma cells. TMZ-induced senescence was triggered by the specific DNA lesion O⁶MeG and characterized by arrest of cells in the G2/M phase. Inhibitor experiments revealed that TMZ-induced senescence was initiated by damage recognition through the MRN complex, activation of the ATR/CHK1 axis of the DNA damage response pathway, and mediated by degradation of CDC25c. TMZ-induced senescence required functional p53 and was dependent on sustained p21 induction. p53-deficient cells failed to induce senescence but were still able to induce a G2/M arrest. p14 and p16, targets of p53, were silenced in our cell system, and did not seem to play a role in TMZ-induced senescence. In addition to p21, the NF-κB pathway was required for senescence, which was accompanied by induction of the senescence-associated secretory phenotype (SASP). Upon TMZ exposure, we found a strong repression of the mismatch repair proteins MSH2, MSH6, and EXO1 as well as the homologous recombination protein RAD51, which were downregulated by disruption of the E2F1/DP1 complex. Repression of these repair factors was not observed in G2/M arrested p53-deficient cells and therefore represents a specific trait of TMZ-induced senescence.

Running title

Mechanisms of methylating anticancer drug induced senescence

Significance

Findings reveal the mechanism by which the anticancer drug temozolomide induces senescence and downregulation of DNA repair pathways in glioma cancer cells.

Keywords

DNA damage, temozolomide, glioblastoma, senescence, DNA repair, E2F1, p21, G2/M arrest

The authors declare no potential conflicts of interest.

Introduction

The success of cancer therapy with genotoxic anticancer drugs rests on their potency to induce cell death. However, genotoxic anticancer drugs not only induce death, but are also effective in activating other pathways such as cellular senescence, which allows cancer cells to survive without proliferation (1). In a previous study, we have shown that glioblastoma cells treated with the methylating anticancer drug temozolomide (TMZ) undergo apoptosis and, in the same dose range and time period, senescence (2). Evidence for induction of senescence by TMZ was also provided in other studies with glioma cells (3-5). The finding that not all tumor cells can be killed through anticancer drug treatment is of importance in view of the dismal prognosis of glioblastoma patients with a median survival of 14.6 months and the 2-year survival rate less than 26.5% (6).

Temozolomide (TMZ, Temodal®, Temodar®) is being used as first-line monotherapeutic in glioblastoma therapy, applied after resection and usually concomitant with radiotherapy (6). TMZ exerts its cytotoxic effect by the induction of *O*⁶-methylguanine (*O*⁶MeG), which ultimately leads to the formation of DNA double-strand breaks (DSB) and cell death (7). The success of glioma therapy is strongly determined by the DNA repair capacity of a tumour. Thus, the cytotoxic DNA lesion *O*⁶MeG is subject to repair by the DNA repair enzyme *O*⁶-methylguanine-DNA methyltransferase (MGMT). In the absence of MGMT, *O*⁶MeG persists in the DNA and mispairs with thymine during DNA replication, resulting in GC->AT transition mutations. In addition to its mutagenic potential, *O*⁶MeG can be converted *via* DNA replication and futile DNA mismatch repair (MMR) into DSB in the second replication cycle after TMZ exposure. If these DSB are not repaired, they result in chromosomal aberrations and the activation of cell death pathways (7). DSB can be repaired by homologous recombination (HR) and/or non-homologous end joining (NHEJ). The repair of radiation-induced DSB occurs mainly *via* NHEJ, while TMZ-induced DSB are repaired by HR (8). Cells that are neither proficient for MGMT nor HR are highly sensitive to TMZ (8), while cells that express MGMT and lack MMR are resistant (7).

As shown by extensive *in vitro* studies, TMZ-induced death of glioma cells results mainly from apoptosis (9-11). However, TMZ was also shown to induce at the same time autophagy and senescence (2). Senescence induced by TMZ was suggested to be dependent on p53 and CHK1/CDC25c dependent G2/M arrest (3,4). TMZ also induces apoptosis and senescence in glioma cells cultured as multicellular spheroids (5). The role of DNA damage-induced senescence in glioblastoma therapy is less clear. It is pertinent to speculate that senescent cancer cells escape therapy and contribute to recurrent tumor growth, which usually occurs following glioma radio-chemotherapy. Senescence was initially described as a

permanent cell cycle arrest involved in limiting the lifespan of cultured human fibroblasts (12). Contrary to quiescence, which is defined as a temporary cell cycle arrest, senescence cannot be reversed by proliferative stimuli. This general statement is however doubted by recent publications, showing that under specific conditions, cells could escape senescence (13-15). Cellular senescence is induced by telomere shortening (replicative senescence), proliferation-associated signals (oncogenic senescence) or by genomic damage caused, among others, by anticancer drugs (DNA damage-triggered senescence). In the latter case, senescence is dependent on sustained DNA damage response (DDR) signalling, provoked very likely by unreparable DNA damage (16).

As senescence may have a serious impact on therapy, we attempted to study in more detail the mechanism of TMZ-induced senescence in glioma cells. In extension of our previous work (2), we analyzed the impact of the specific TMZ-induced DNA lesion O^6 MeG and the DDR triggered by this critical lesion on the induction of cell cycle arrest and senescence. Furthermore, we addressed the question whether in TMZ-induced senescent glioma cells the DNA repair capacity is altered compared to non-senescent cells. The data show that the TMZ-induced DNA damage O^6 MeG is the main trigger of senescence, which is initiated by activation of the MRN-ATR-CHK1 pathway and dependent on CDC25c degradation. In addition to this, activation of p21 and NF- κ B is required, but not of p14 or p16. TMZ-induced senescence was accompanied by disruption of the E2F1/DP1 complex, which leads to downregulation of the DNA repair factors EXO1, MSH2, MSH6 and RAD51. The high potency of the TMZ-induced damage O^6 MeG to trigger senescence may explain the lack of curability of gliomas treated with this anticancer drug.

Material and Methods

Cell culture, drug treatment and siRNA-mediated knockdown

The glioma cell lines (LN229 (RRID:CVCL_0393), LN229-MGMT, U87 (RRID:CVCL_0022), LN308 (RRID:CVCL_0394) and U138 (RRID:CVCL_0020)) were cultivated in Dulbecco's minimal essential medium (DMEM) containing 10% fetal bovine serum (FBS) in a humidified atmosphere containing 7% CO₂ at 37°C. U87 cells were purchased from Cell Line Service (Eppelheim, Germany) and the glioblastoma cell line LN229 was obtained from LGC Standards (Wesel am Rhein, Germany). Both cell lines are deficient for MGMT expression due to promoter methylation and also show no MGMT activity as determined by the radioactive MGMT assay (17). LN229-MGMT cells were stably transfected with MGMT cDNA showing strong MGMT expression and activity (2). All cell lines were regularly checked for

MGMT activity. LN308 and U138 cells were kindly provided by Prof. Weller (Laboratory of Molecular Neuro-Oncology, University Hospital and University of Zurich, Switzerland) and were characterized (18). MGMT transfected LN229 cells were described previously (2).

All cells were kept in culture for no longer than 2 month and were regularly checked for mycoplasma contamination using the VenorGEM classic detection kit (#11-1100) from Minerva Biologicals. All lines were characterized in the laboratory of origin, displayed the expected phenotype, but were not reauthenticated in our laboratory.

TMZ was purchased from Prof. Geoff Margison, Centre for Occupational and Environmental Health, University of Manchester, GB. The NF- κ B inhibitors III (CAS 380623-76-7, Merck Millipore) and JSH23 (CAS 749886-87-1, Selleckchem) were used at 10 μ M and 50 μ M respectively. The CHK1 inhibitor UCN-01 (CAS 112953-11-4, Sigma Aldrich) was used at 50 nM, the CHK1 inhibitor MK8776 (CAS 891494-63-6, Selleckchem) was used at 0.5-2 μ M, the CHK2 inhibitor II hydrate (CAS 516480-79-8, Sigma Aldrich) was used at 10 μ M and the p21 inhibitor UC2288 (CAS 532813, Calbiochem) was used at 5 μ M. The ATM inhibitor KU60019 (CAS 925701-49-1, Selleckchem) was used at 10 μ M, the ATR inhibitor VE-821 (CAS 1232410-49-9, Selleckchem) was used at 10 μ M, the DNA-PKcs inhibitor KU0060648 (CAS, 881375-00-4, Selleckchem) was used at 900 μ M and the MRN inhibitor Mirin (CAS 1198097-97-0 Tocris) was used at 25 μ M. For silencing of p21, predesigned siRNA (sc-29427, Santa Cruz) and control human non-silencing siRNA (Silencer Select Predesigned siRNA Negative Control #1 siRNA; Ambion) were used. Silencing of CHK1 was performed using 100 nmol/L predesigned siGENOME SMARTpool siRNA (M-003255-04, Dharmacon). The transfections of siRNAs were performed using Lipofectamine RNAiMAX Reagent (Invitrogen).

Xenograft experiments: To induce subcutaneous xenografts, U87 cells (2.5×10^6) were injected in the left and the right flank of four female immunodeficient mice (BALB/cAnNRj-*Foxn1^{nu/nu}*, Janvier Labs). When tumours reached a suitable size (22 mm³), two randomly selected animals were injected with TMZ (200 mg/kg body weight in DMSO/NaCl i.p.) and two with solvent, respectively. 96 h later the mice were sacrificed and tumours were isolated, immediately frozen in liquid nitrogen and stored at -80°C. For expression analysis, the left and right tumour were combined and the tissue was disintegrated using a tissue lyser (Retsch). Whole cell protein extract was isolated as described (19) and concentration was measured according to the Bradford method. Animal experiments were performed in accordance with relevant institutional and national guidelines and regulations, and were approved by the Landesuntersuchungsamt Rheinland Pfalz, Germany (23 177-07 / 041-15V2).

Preparation of RNA and RT qPCR: Total RNA was isolated using the Nucleo Spin RNA Kit (Machery and Nagel, Düren, Germany). One μg total RNA was transcribed into cDNA (Verso cDNA Kit, Thermo Scientific) and qPCR was performed using the GoTaq[®] qPCR Master Mix Protocol (Promega, Madison, USA) and the CFX96 Real-Time PCR Detection System (Biorad, München, Germany). In all experiments, qPCR was performed in technical triplicates, SD shows intra-experimental variation. The analysis was performed using CFX Manager[™] Software. Non-transcribed controls were included in each run, expression was normalized to *gapdh* and *β -actin*; the untreated control was set to one. The specific primers are listed in Supplementary Table S1.

Immunoprecipitation and Chromatin immunoprecipitation (ChIP): Immunoprecipitation was performed using the Catch and Release[®] v2.0 Kit (Merck, Darmstadt, Germany) according to the manufacturer's protocol. Chromatin immunoprecipitation was performed as described (20). Real time PCR was performed using specific primers flanking the E2F1 binding site of *EXO1*, *MSH2*, *MSH6*, and *RAD51*, which are listed in Supplementary Table S1.

Determination of apoptosis and cell cycle progression: For monitoring drug-induced apoptosis, annexin V-FITC / propidium iodide (PI) double stained cells were analyzed by flow cytometry. To determine cell cycle distribution, cells were incubated for different times after TMZ exposure. Harvested samples were prepared as follows. Following 30 min RNA digestion with 0.1 mg/mL RNase in PBS, they were stained with propidium iodide (PI) and cell cycle distribution was determined by flow cytometry using a BD FACSCanto[™] II. Experiments were repeated at least three times, mean values \pm SD are shown.

Determination of senescence and isolation of senescent cells. For detection of senescence, cells were washed twice with PBS, afterwards fixed with 2% formaldehyde, 0.2% glutaraldehyde in PBS. After washing with PBS, cells were stained (40 mM citric acid/phosphate buffer pH 6.0, 150 mM NaCl, 2 mM MgCl₂, 5 mM potassium ferrocyanide, 5 mM potassium ferricyanide, 0.1% x-Gal) overnight at 37°C. Cells were then washed with PBS and overlaid with 70% glycerine. Micrographs were acquired and analyzed using the Cell A Imaging software (Olympus) in combination with a Zeiss Axiovert 35 microscope. 500-1000 cells were analyzed per sample. In all cases, experiments were repeated at least three times; mean values \pm SD are shown. For flow cytometry-based detection of senescence, cells were exposed to TMZ for indicated times. Thereafter medium was removed and 4 ml fresh medium containing 10% FCS and 300 μM chloroquine was added per 10-cm dish. Cells were incubated for 30 min at 37°C. Finally 33 μM C₁₂FDG (ImaGene Green[™] C12FDG lacZ Gene Expression Kit) was added and incubated for 90 min at 37°C. The medium was

removed, cells were PBS-washed, trypsinized and resuspended in PBS. Senescence was measured at the BD FACSCanto™ II flow cytometer. For isolation of senescent cells, the cells were resuspended in dissociation buffer (Gibco) containing 1% FCS and C₁₂FDG positive cells were sorted using a BD FACSAria sorter.

Preparation of protein extracts and western blot analysis: Whole-cell and nuclear extracts were prepared as previously described (19). For western blot analysis using phospho-specific antibodies, cells were directly lysed in 1x SDS-PAGE sample buffer and subsequently sonified. Mouse mAb were diluted 1:500-1:1000 in 5% BSA, 0.1% Tween-TBS and incubated overnight at 4°C. Rabbit pAb were diluted 1:2000 and incubated 2h at RT. The protein-antibody complexes were visualized by Pierce® ECL Western Blotting Substrate (Thermo Fisher). The specific antibodies are listed in Supplementary Table S2.

Mismatch Repair (MMR) and homologous recombination (HR) activity assay. For MMR-specific electromobility shift assay, 29-nucleotide oligomers with the sequence 5'-GGGCTCGAGCTGCAGCTGCTAGTAGATCT-3' were annealed to oligomers with the sequence 5'-GGGAGATCTACTAGNAGCTGCAGCTCGAG-3' (n= C or T) and labelled with [32P]dATP using polynucleotide kinase. Nuclear extracts were prepared and incubated with the oligomers as previously described (21). DNA-protein complexes were separated in 4% polyacrylamide gels. The efficiency of HR was determined by a qPCR-based HR Assay kit (Norgen Biotek Corporation, ON, Canada), as described (11). Cells were exposed to 100 μM TMZ, 72 h later the cells were transfected with the HR plasmids and 24 h thereafter subjected to isolation of total cellular DNA. Samples were standardized with universal primers, detecting the plasmid backbone for control of transfection efficiency.

Quantification and statistical analysis. The data were evaluated using Student's t-test and were expressed as a mean ± SD. * $p \leq 0.05$ was considered statistically significant, ** $p \leq 0.01$ very significant, *** $p \leq 0.001$ highly significant and **** $p \leq 0.0001$ most significant. Statistical analyses were performed using GraphPad Prism version 6.01 for Windows, GraphPad Software, La Jolla California USA (www.graphpad.com).

Results

Senescence following TMZ is dependent on O⁶MeG and triggered by the MRN-ATR pathway
Previously we showed that O⁶MeG is the initial trigger of TMZ-induced apoptosis, which is mediated through the DDR (22). To analyze whether this is also true for the activation of

senescence, the DDR factors ATM, ATR, MRN and DNA-PKcs were pharmacologically inhibited and the frequency of senescence was measured in LN229 cells (proficient for p53 and deficient for MGMT) by scoring senescence associated β -Gal positive cells (Fig. 1A). In order to identify the primary DNA damage triggering senescence, activation of senescence was also measured in LN229 cells that express MGMT following transfection with MGMT cDNA (LN229-MGMT). The data show that senescence was induced only in MGMT deficient LN229 glioma cells, but not in the MGMT proficient LN229-MGMT isogenic cell line (Fig. 1A). Since the isogenic lines differ only in the MGMT repair capacity and, thereby, the amount of O⁶-MeG following TMZ treatment, we conclude that this lesion is not only responsible for inducing TMZ-induced cell death (9), but also for senescence. The inhibitor experiments revealed that TMZ-induced senescence in MGMT deficient cells is dependent on ATR, but not ATM. In addition to ATR, inhibition of MRN and DNA-PKcs also protected against TMZ-induced senescence, indicating the MRN complex and DNA-PKcs being involved.

TMZ-induced senescence is activated in the G2/M cell cycle phase

To mimic the clinical situation, repeated exposure to TMZ (25 and 50 μ M) at five consecutive days was performed. In addition, a combined treatment schedule using TMZ (25 μ M) and IR (2 Gy) was applied. The data revealed that repeated low-dose TMZ exposure is highly efficient in inducing senescence in p53 proficient U87 (up to 60%) and LN229 (up to 80%) cells (Fig. 1B). Importantly, IR exposure did not influence senescence induction through TMZ. Senescence was also activated upon single TMZ exposure in a dose- and time-dependent manner, starting 72 h after treatment with 25 μ M TMZ in U87 (Fig. 1C) and LN229 cells (Fig. 1D), reaching 40-50% after 144 h following exposure with 100 μ M TMZ.

Compared to the high level of senescence, apoptosis and necrosis were induced at low levels (up to 20%) upon repeated treatment of U87 (Fig. 1E) and up to 10% necrosis and 25% apoptosis upon single exposure (Fig. 1F). Also in LN229 cells repeated treatment induced up to 20% apoptosis and necrosis (Fig. 1G) and single exposure induced up to 15% apoptosis and necrosis (Fig 1.H).

The data indicate that senescence (as determined by β -gal positivity) is the major endpoint induced by TMZ followed by activation of cell death pathways. Of note, the strong activation of senescence by TMZ was not affected by increased FCS-dependent proliferation stimuli since TMZ induced a comparable frequency of senescence (as well as necrosis and apoptosis) in cells cultivated in 10% or 1% serum (Supplementary Fig. S1A-C). Since both chronic (Fig. 1E/G) and single exposure (Fig. 1F/H) induced a strong G2/M arrest (>75%), we infer that TMZ-induced senescence occurs in the G2/M cell cycle phase, which was also supported by the complete G2/M-arrest observed in FACS-isolated senescent cells (see below).

TMZ-induced senescence is dependent on p21

An important pathway in activating cell cycle arrest and senescence was shown to be triggered by p53-mediated induction of p21. The p53 wt glioma cell lines used in this study display a strong phosphorylation of p53 at Ser15 and the induction of p21 following TMZ exposure (Fig. 2A). Contrary to U87 and LN229 cells, the p53 deficient LN308 and the p53 mutated U138 cells did not show p21 induction upon TMZ exposure, neither on protein (Fig. 2B) nor on mRNA level (Fig. 2C). We should note that in p53 mutated U138 cells phosphorylation of p53 on Ser15 can be detected, which results however in a transcriptionally inactive protein. In line with the p53/p21 status, LN308 and U138 cells neither showed TMZ-induced cell death (Supplementary Fig. S2A) nor senescence (Fig. 2D) in the dose range of up to 100 μ M. Contrary to senescence, the TMZ-induced G2/M arrest was independent of p53 and p21 (Fig. 2E). This suggests that upon TMZ treatment, senescence, but not the G2/M arrest, is dependent on p21. In line with this, knockdown of p21 (Supplementary Fig. S2B) completely abrogated the induction of senescence (Fig. 2F), but did not abrogate the G2/M arrest (Fig. 2G).

TMZ-induced G2/M arrest results from CHK1 dependent CDC25c degradation

The G2/M transition is regulated by the CDK1/CyclinB complex. During the G2 phase of the cell cycle, CDK1 is maintained in an inactive state due to WEE1 dependent phosphorylation at Tyr15. Activation of the CDK1/CyclinB complex and entry into mitosis is mediated via CDC25c mediated Tyr15 dephosphorylation and CDK activating kinase (CAK)-mediated phosphorylation at Thr161. Concerning the DNA damage-induced G2/M arrest, it has been shown that CHK1 can phosphorylate CDC25c at Ser216 leading to nuclear export of CDC25c (23). It has also been shown that doxorubicin, camptothecin and topotecan can induce a G2/M arrest via CHK1 dependent CDC25a degradation (24,25). We observed in U87 and LN229 cells a strong phosphorylation of CHK1 and CHK2 48 to 96 h after TMZ treatment (Fig. 3A). In parallel, a significant reduction in CDC25c protein (Fig. 3A) and an accumulation of cells in the G2/M phase was observed (Supplementary Fig. S2C), while CDC25a remained unchanged. In line with the degradation of CDC25c, CDK1 remained inactive, as indicated by the missing (U87) or weak (LN229) dephosphorylation of CDK1 at Tyr15 (Supplementary Fig. S2D). Finally, a strong nuclear retention of the cyclinB1 complex was observed, further showing that the CDK1/cyclinB1 complex is kept in an inactive state (Supplementary Fig. S2E).

To elucidate whether CHK1 and CHK2 are responsible for the reduced expression of CDC25c and the activation of the G2/M arrest, both factors were pharmacologically inhibited. Whereas inhibition of CHK1 counteracted the reduction in CDC25c protein (Fig. 3B) and

prevented the G2/M arrest (Fig. 3C), inhibition of CHK2 and of p21 did not affect CDC25c protein level and only caused a minor reduction in the G2/M arrest (Fig. 3C). *Vice versa*, inhibition of p21 and, to a lesser extent, CHK1, but not CHK2, abrogated senescence (Fig. 3D). Similar results were obtained using a second CHK1 inhibitor and CHK1-specific siRNA (Supplementary Fig. S3A-D). To address the impact of the initial DDR kinases on the G2/M arrest, ATM, ATR, MRN and DNA-PK_{cs} were inhibited and the cell cycle distribution was measured in LN229 cells (Fig. 3E). The data show, that similar to senescence, the G2/M arrest is dependent on ATR, but not ATM. Interestingly, in this case, inhibition of MRN and DNA-PKcs did not prevent the G2/M arrest. Since MGMT expressing cells did not display a G2/M arrest, it is obvious that the observed cell cycle arrest is triggered by the specific DNA lesion O⁶MeG.

Maintenance of TMZ-induced senescence is mediated through NF-κB

Senescence can be divided into two phases, initiation and maintenance (26). To render senescence irreversible, further cellular changes have to occur. During the maintenance phase, the cell cycle arrest becomes irreversible (13), mainly through the accumulation of p14 and p16. Furthermore it was reported that either p14 or p16 or both can take over the role of p21 in maintaining senescence. In this context, it is important to note that up to 50% of gliomas show a deletion of p14/16 (27). Among the cell lines used in our study, U87, U138 and LN229 harbour a deletion in exon 1 of CDKN2A as indicated by methylation-specific PCR (MSP) detecting both the unmethylated and the methylated exon 1 (Supplementary Fig. S4A,B) and show no p14/p16 expression (Supplementary Fig. S4C), while LN308 cells are p14/p16 proficient. Interestingly, LN308 cells do not show TMZ-induced senescence, which is not supporting the view that p14/p16 can substitute for p21, at least in the process that leads to TMZ-induced senescence of glioma cells.

Mechanisms maintaining senescence were reported to depend on an NF-κB-dependent amplifying loop, leading to enhanced ROS production (28). To analyze the impact of NF-κB on TMZ-induced senescence, expression of the NF-κB inhibitor IκB was analyzed (Fig. 4A). IκB protein level was strongly reduced 48 h after TMZ in U87 and LN229 cells, indicating activation of NF-κB. This was further supported by reporter assays showing enhanced NF-κB activity upon TMZ exposure (Supplementary Fig. S5A). A clinically relevant mechanism triggered by NF-κB is the senescence-associated secretory phenotype (SASP), which is characterized by the induction and secretion of different cytokines (29). In order to analyze whether TMZ can induce SASP, the time-dependent expression of the inflammatory cytokines IL-6 and IL-8, which are main components of SASP, were analyzed in U87 and LN229 cells. The data clearly show that TMZ induces the expression of *IL6/IL8* mRNA (Supplementary Fig. S5B) and augments the production of IL-6 and IL-8 in glioma cells (Fig.

4B). In order to investigate the role of NF- κ B in TMZ-induced senescence, NF- κ B was pharmacologically inhibited. The inhibitor was added for 48 h and senescence was analyzed 144 h after TMZ exposure *via* β -Gal staining and flow cytometry-based measurement of C₁₂FDG positive cells (Fig. 4C). For verification, the experiments were repeated using an alternative NF- κ B inhibitor (Supplementary Fig. S5C). The results showed a dramatic reduction in TMZ-induced senescence following NF- κ B inhibition (Fig. 4C). Interestingly, these experiments also revealed an increase in apoptosis (Fig. 4D), indicating that NF- κ B might be important in triggering the switch between TMZ-induced senescence and apoptosis. To analyze the impact of NF- κ B on the expression of anti-apoptotic factors, the expression of c-IAP2, Bcl-X_L, Survivin and XIAP, known transcriptional targets of NF- κ B, were determined. The data indicate a strong time-dependent induction of c-IAP2 and a weak induction of Bcl-X_L and XIAP (Supplementary Fig. S5D). Survivin expression was not induced. Induction of c-IAP2 and Bcl-X_L was significantly reduced by NF- κ B inhibition (Fig. 4E), suggesting that these factors are involved in apoptosis prevention upon TMZ exposure.

TMZ induces senescence-associated transcriptional repression of DNA repair factors

To elucidate whether TMZ-induced senescence alters the cellular DNA repair capacity, we analyzed the expression of various DNA repair factors involved in the resistance against TMZ on RNA level. Thus, we observed that several DNA repair genes, including the MMR genes *EXO1*, *MSH2*, *MSH6* and an important component of HR, namely *RAD51*, are transcriptionally repressed following TMZ exposure. All four genes showed reduced expression starting 48 h after exposure to 100 μ M TMZ in LN229 and U87 cells (Fig. 5A), whereas the p53 target gene *DDB2* was upregulated. Next, we analyzed the impact of transcriptional repression on the corresponding proteins. The data show that reduced transcription resulted in decreased MSH2, MSH6, EXO1 and RAD51 protein expression, both following single (Fig. 5B) and repeated TMZ exposure (Fig. 5C). The reduced mRNA and protein levels had an impact on the cellular repair capacity, as shown by decreased MMR binding activity (Fig. 5D) and reduced HR activity (Fig. 5E) upon TMZ treatment.

TMZ-induced transcriptional repression of EXO1, MSH2, MSH6 and RAD51 is mediated by decreased E2F1/DP1 signalling

Since ChIP-Seq and ChIP-chip studies have described *EXO1*, *MSH2*, *MSH6* and *RAD51* as potential targets of E2F1 and E2F4 (30,31), we analyzed the role of E2F1 in the repression of *EXO1*, *MSH2*, *MSH6* and *RAD51*. Thus, we measured the expression of E2F1 and its binding partners DP1 and RB as well as E2F1 phosphorylation on protein level upon single and chronic TMZ exposure. The data (shown in Supplementary Fig. S6A-D) revealed only minor alterations in the overall protein levels of E2F1, DP1 and RB. Only upon chronic

exposure of U87 cells a decrease of DP1 protein was observed. Similarly, the phosphorylation of E2F1 at Ser³³⁷ (target of CDK4/6, enhancing transcriptional activity) and Ser³⁶⁴ (target of CHK2) was not altered upon TMZ exposure.

Since the activity of E2F1 strongly depends on its interaction with DP1, we analyzed the complex formation between E2F1 and DP1 via co-immunoprecipitation. The results clearly show that the complex between E2F1 and DP1 was disrupted by TMZ, both upon single and chronic exposure (Fig. 6A/B). Finally, we analyzed the binding of E2F1 and DP1 to the promoter of *EXO1*, *MSH2*, *MSH6* and *RAD51* using ChIP. Binding of E2F1 (Fig. 6C), and even more pronounced of DP1 (Fig. 6D) to the corresponding promoters was strongly reduced 48h and 72h following TMZ exposure, indicating that these genes are silenced due to lack of activation by E2F1/DP1.

Next, we addressed the question of whether gene silencing is a direct response to the G2/M arrest or whether it is associated with senescence. As shown in Fig. 2, U138 and LN308, showed a strong G2/M arrest, without inducing senescence. Despite the G2/M arrest, these cells showed no reduction in the expression of *EXO1*, *MSH2*, *MSH6* or *RAD51* (Supplementary Fig. S6E), indicating that the repression is not directly caused by the G2/M arrest, but might be associated with the p21-induced senescence phenotype. This assumption was supported by the finding that siRNA-mediated knockdown of p21 did not only prevent senescence, but also abrogated the repression of *EXO1*, *MSH2*, *MSH6* and *RAD51* (Fig. 6E).

TMZ-induced transcriptional repression of EXO1, MSH2, MSH6 and RAD51 occurs in senescent cells

To further support the hypothesis that the TMZ-induced repression of *EXO1*, *MSH2*, *MSH6* and *RAD51* is a specific feature of senescent cells, TMZ-induced senescent cells were separated by flow cytometry using C₁₂FDG for labelling. The frequency of senescence in the sorted cells as well as in unsorted cells exposed or not exposed to TMZ was verified microscopically by β -Gal staining, showing that the FACS enriched cell population contained ~95% senescent cells (Fig. 7A/B, left diagram). Moreover, cell cycle distribution was measured, revealing that ~90% of the C₁₂FDG isolated senescent cells were arrested in the G2/M phase of the cell cycle (Fig. 7 A/B, middle diagram), clearly showing that TMZ-induced senescent cells are arrested in the G2/M phase. Finally, the expression of *EXO1*, *MSH2*, *MSH6* and *RAD51* was analyzed in C₁₂FDG sorted cells. The data show strongly reduced protein levels of these proteins in the senescent population (Fig. 7 A/B, right diagram).

Repression of EXO1, MSH2, MSH6 and RAD51 in mouse xenografts treated with TMZ

To determine whether TMZ also reduces the expression of EXO1, MSH2, MSH6 and RAD51 in glioma cells grown in a host *in vivo*, U87 cells were injected into immunodeficient mice. As shown in Fig. 7C, TMZ treatment of mice clearly reduced EXO1, MSH2, MSH6 and RAD51 protein, as well as CDC25c protein level. Furthermore, the protein level of I κ B decreased and the level of p21 increased following systemic TMZ treatment. Thus, the same phenotype was observed *in vivo*, supporting the notion that TMZ has the potency to trigger senescence in tumors, which is accompanied by down-regulation of the repair pathways referred to above.

Discussion

The therapy of high-grade gliomas rests on treatment with the anticancer drug TMZ, which is highly effective in inducing apoptosis (9). However, at treatment-relevant doses not all cells are killed by apoptosis, which is likely the reason why TMZ treatment can only extend the median survival of patients from 12.1 up to 14.6 months (6). Activation of apoptosis through TMZ is triggered by the minor DNA lesion O⁶MeG and subsequent activation of the DDR (22). Using synchronized cells, we further showed that O⁶MeG triggers the accumulation of cells in the G2/M phase of the post-treatment cell cycle (32). Besides inducing cell death through apoptosis, TMZ activates also survival pathways such as DNA repair, autophagy and senescence (2). It appears that apoptosis is only a minor pathway, while senescence represents a dominant trait triggered by TMZ in glioblastoma cells.

Hallmarks of cellular senescence are activation of the DDR and subsequent induction of a cell cycle arrest. During replicative and oncogenic senescence as well as following exposure to most genotoxic agents, senescent cells are arrested in the G1 phase. This is in contrast to our finding that TMZ induces senescence in the G2/M phase. Data concerning the activation of senescence in the G2 phase of the cell cycle are limited (33). In normal human cells, the G2/M arrest and subsequent senescence were analyzed following treatment with the topoisomerase II inhibitor ICRF-193. In this system, the G2/M arrest depends on p21, which was associated with nuclear retention of CyclinB1, as well as with the accumulation of RB (34). Furthermore, p21 has also been shown to sequester inactive CyclinB1-Cdk1 complexes in the nucleus of ICRF-193 exposed human fibroblasts (35-37). In contrast to this, in human HCT-116 or U2OS cancer cells, no nuclear retention of CyclinB1 was observed during DNA damage-induced G2/M arrest (38). The discrepancy between normal and cancer cells was explained by the fact that HCT-116 or U2OS cells, besides being p53-proficient, show inefficient and late p21 activation after treatment with ICRF-194 or the radiomimetic drug bleomycin (39).

According to our study, activation of the G2/M arrest and senescence is triggered by the specific DNA damage O⁶MeG. It is important to note that induction of the G2/M arrest occurs in both p53 proficient and p53 deficient cells. The G2/M arrest was completely abrogated upon inhibition of CHK1, but not p21, clearly indicating that induction of the G2/M arrest in TMZ-exposed glioma cells is independent of p21. According to our findings, activation of the TMZ-induced G2/M arrest occurs through the CHK1-dependent degradation of CDC25c and the subsequent lack of CDK1 activation. This is in line with a report showing that dysfunctional telomeres activate DDR and promote CHK1/CHK2-dependent phosphorylation of CDC25c at Ser216 leading to its proteasomal degradation and the induction of the G2/M arrest (40). In contrast to the G2/M block induced by dysfunctional telomeres, the TMZ-induced G2/M arrest appears to depend only on ATR and CHK1 and not on ATM and CHK2. Furthermore, our findings confirm data that highlight the importance of CHK1 activation for inducing the TMZ-induced G2/M arrest in glioma cells (3,4).

Upon activation of the G2/M arrest, p21 appears to be crucial for rendering the cell cycle arrest irreversible and activating the senescent phenotype. The exact mechanism by which p21 induces TMZ-induced senescence is however still unclear. Contrary to data obtained in HCT-116 or U2OS cancer cells (38,39), we observed a strong and long-lasting nuclear retention of CyclinB1 after TMZ treatment, suggesting that p21-dependent sequestration of inactive CyclinB1-CDK1 complexes may be important for p21-mediated endurance of the TMZ-induced G2/M arrest and senescence. Besides p21 also NF- κ B signalling is important for TMZ-induced senescence. Thus we provide evidence that TMZ exposure leads to the degradation of the NF- κ B inhibitor I κ B, activation of NF- κ B and the upregulation of NF- κ B targets such as IL-6 and IL-8. Interestingly, we observed that inhibition of NF- κ B abrogates senescence and shifts cells into apoptosis. In parallel, a strong induction of the anti-apoptotic NF- κ B target BIRC3/c-IAP2 was observed after TMZ treatment. Since BIRC3/c-IAP2 induction was abrogated by NF- κ B inhibition, we suppose that this factor might be causally involved in the protection against TMZ-induced apoptosis. This is in line with data showing that BIRC3/c-IAP2 up-regulation results in apoptosis evasion and therapeutic resistance in glioblastoma (41). All together our data suggests that NF- κ B supports senescence by activation of SASP, which is thought to maintain senescence, and/or NF- κ B dependent activation of anti-apoptotic factors and thereby abrogation of cell death.

Studying the DNA repair status in TMZ-induced senescent cells, we observed that the MMR genes *EXO1*, *MSH2*, *MSH6* and the rate-limiting factor of HR, *RAD51*, are transcriptionally repressed. This was accompanied by low-level expression of the corresponding proteins and diminished DNA repair capacity. As indicated by immunoprecipitation and ChIP experiments, repression of these genes was caused by the disruption of the E2F1/DP1 complex. The data

showing E2F1-dependent regulation of MSH2 and MSH6 are in line with the previous observation that E2F1 can regulate MSH2 and MSH6 in rat cells (42). They are also compatible with the finding that embryonal stem cells of mice show a higher expression of MSH2 and MSH6 compared to differentiated cells due to increased E2F1 activity (43). Corresponding to the fact that MMR and HR are needed in S/G2, a higher expression of MSH2 and RAD51 has been described in these cell cycle phases (44). Here we describe for the first time a nearly complete repression of these factors and, in addition to these, of MSH6 and EXO1 upon genotoxic stress. The transcriptional repression in TMZ-treated glioma cells is not caused by an arrest in G0/G1 and also not by accumulation of cells in G2/M *per se*, since the repression of these repair proteins cannot be observed in G2/M-arrested p53 deficient cells. The repression strongly depends on the induction of p21-mediated senescence. The finding that senescent cells isolated by FACS showed strongly reduced expression of *EXO1*, *MSH2*, *MSH6* and *RAD51* support the idea that repression of these repair factors is part of the SASP.

We are aware of the fact that non-replicating senescent glioma cells are necessarily refractory to killing by TMZ, since O⁶MeG adducts need replication in order to be converted into killing lesions (7). Therefore, the downregulation of repair proteins has presumably no direct impact on TMZ resistance. However, we consider the possibility that as a result of impaired DNA repair capacity, including the HR pathway, DSB induced by concomitant radiotherapy and other types of spontaneously arising DNA damage will not be repaired in an error-free way in senescent cells. This may lead to further genomic alterations, which could contribute to increased aggressiveness of recurrent tumors once senescent cells become reactivated. Can this happen?

Commonly, senescence is considered to be a clinically favourable response to chemotherapy because it is thought to permanently block the proliferation of tumour cells and, therefore, stop tumour growth. However, several studies provided hints that cells can escape from genotoxin-induced senescence (13-15). In addition, regrowth experiments following TMZ treatment have been performed in U87 cells showing restart of growth one week after TMZ exposure (45). However, these experiments could not prove convincingly regrowth of senescent cells. The question concerning reversibility of TMZ-induced senescence is therefore of central importance and has to be urgently addressed in future experiments.

Another question that remains to be solved is whether the expression of *EXO1*, *MSH2*, *MSH6* and *RAD51* recovers once glioma cells escape from senescence, or whether the long-lasting transcriptional repression results in epigenetic silencing via histone modifications or CpG methylation. The latter hypothesis gains support from the findings that reduced MMR

activity was observed in melanomas after exposure to TMZ (46) and significantly lower MLH1, MSH2, MSH6 and PMS2 protein levels were observed in recurrent glioblastomas (47,48). Importantly, it was shown that the MSH2 and MSH6 levels are quantitatively related to the sensitivity of cells to methylating agents (49) and that even minor changes in the expression of MSH2 can have an impact on the response of gliomas to TMZ (50). Another open issue pertains to the question of selective killing of senescent cells and drug-induced reactivation of senescent cells, considering the possibility of improving the efficacy of TMZ. Some of these modifying drugs like resveratrol were shown to act via reinforcing the TMZ-induced senescence in glioma cells (51). Based on our and previously published data (52), also senolytic drugs may improve TMZ-based therapy of malignant glioma. Drug combinations targeting in a specific way both the senescence and the apoptosis pathway should be tested in future studies.

In summary, TMZ induces senescence at high level in glioma cells. This scenario is outlined in Fig. 7D. The arrest in the G2/M phase of the cell cycle is initiated *via* ATR/CHK1-mediated degradation of CDC25c leading to abrogated CDK1/CyclinB1 activity and is further fixed into senescence *via* p21. Furthermore, there is growing evidence that NF- κ B is important for TMZ-induced senescence. In this process, NF- κ B could act by induction of anti-apoptotic factors, thereby suppressing the apoptotic pathway and/or by induction of the SASP. Concomitant to senescence, a transcriptional repression of *EXO1*, *MSH2*, *MSH6* and *RAD51* was observed, which is mediated by disruption of the E2F1/DP1 complex. Therefore, reduced MMR and HR capacity can be considered a specific phenotype of TMZ-induced senescence, which could enhance the aggressiveness of these cells, by allowing additional mutational and genomic alterations. These alterations may facilitate escape from senescence and thereby contribute to the formation of therapy resistant recurrences.

Acknowledgements

This study was funded by grants of the Wilhelm Sander Stiftung (AZ – 2014.102.1) and the German Science Foundation [DFG CH 665/6-1] to Markus Christmann, by a grant of the German Cancer Aid (Mildred Scheel Foundation, AZ – 111404) to Maja T. Tomicic and Markus Christmann and by a grant of the German Science Foundation (DFG KA724/18-1,2) to Bernd Kaina. We greatly appreciate the technical assistance of Birgit Rasenberger and support by Christian Schwarzenbach. Support by IMB's Flow Cytometry Core Facility is gratefully acknowledged.

Declaration of Interests

The authors declare there are no competing interests.

References

1. Lee M, Lee JS. Exploiting tumor cell senescence in anticancer therapy. *BMB reports* **2014**;47:51-9
2. Knizhnik AV, Roos WP, Nikolova T, Quiros S, Tomaszowski KH, Christmann M, *et al.* Survival and death strategies in glioma cells: autophagy, senescence and apoptosis triggered by a single type of temozolomide-induced DNA damage. *PloS one* **2013**;8:e55665
3. Hirose Y, Berger MS, Pieper RO. Abrogation of the Chk1-mediated G(2) checkpoint pathway potentiates temozolomide-induced toxicity in a p53-independent manner in human glioblastoma cells. *Cancer research* **2001**;61:5843-9
4. Hirose Y, Berger MS, Pieper RO. p53 effects both the duration of G2/M arrest and the fate of temozolomide-treated human glioblastoma cells. *Cancer research* **2001**;61:1957-63
5. Gunther W, Pawlak E, Damasceno R, Arnold H, Terzis AJ. Temozolomide induces apoptosis and senescence in glioma cells cultured as multicellular spheroids. *British journal of cancer* **2003**;88:463-9
6. Stupp R, Mason WP, van den Bent MJ, Weller M, Fisher B, Taphoorn MJ, *et al.* Radiotherapy plus concomitant and adjuvant temozolomide for glioblastoma. *The New England journal of medicine* **2005**;352:987-96
7. Kaina B, Christmann M, Naumann S, Roos WP. MGMT: key node in the battle against genotoxicity, carcinogenicity and apoptosis induced by alkylating agents. *DNA repair* **2007**;6:1079-99
8. Quiros S, Roos WP, Kaina B. Rad51 and BRCA2--New molecular targets for sensitizing glioma cells to alkylating anticancer drugs. *PloS one* **2011**;6:e27183
9. Roos WP, Batista LF, Naumann SC, Wick W, Weller M, Menck CF, *et al.* Apoptosis in malignant glioma cells triggered by the temozolomide-induced DNA lesion O6-methylguanine. *Oncogene* **2007**;26:186-97
10. Tomicic MT, Meise R, Aasland D, Berte N, Kitzinger R, Kramer OH, *et al.* Apoptosis induced by temozolomide and nimustine in glioblastoma cells is supported by JNK/c-Jun-mediated induction of the BH3-only protein BIM. *Oncotarget* **2015**;6:33755-68
11. Christmann M, Diesler K, Majhen D, Steigerwald C, Berte N, Freund H, *et al.* Integrin alphaVbeta3 silencing sensitizes malignant glioma cells to temozolomide by suppression of homologous recombination repair. *Oncotarget* **2017**;8:27754-71
12. Hayflick L. The Limited in Vitro Lifetime of Human Diploid Cell Strains. *Experimental cell research* **1965**;37:614-36
13. Beausejour CM, Krtolica A, Galimi F, Narita M, Lowe SW, Yaswen P, *et al.* Reversal of human cellular senescence: roles of the p53 and p16 pathways. *The EMBO journal* **2003**;22:4212-22
14. Michishita E, Nakabayashi K, Ogino H, Suzuki T, Fujii M, Ayusawa D. DNA topoisomerase inhibitors induce reversible senescence in normal human fibroblasts. *Biochemical and biophysical research communications* **1998**;253:667-71
15. Chitikova ZV, Gordeev SA, Bykova TV, Zubova SG, Pospelov VA, Pospelova TV. Sustained activation of DNA damage response in irradiated apoptosis-resistant cells induces reversible senescence associated with mTOR downregulation and expression of stem cell markers. *Cell cycle* **2014**;13:1424-39
16. d'Adda di Fagagna F. Living on a break: cellular senescence as a DNA-damage response. *Nature reviews Cancer* **2008**;8:512-22
17. Christmann M, Nagel G, Horn S, Krahn U, Wiewrodt D, Sommer C, *et al.* MGMT activity, promoter methylation and immunohistochemistry of pretreatment and recurrent malignant gliomas: a comparative study on astrocytoma and glioblastoma. *International journal of cancer Journal international du cancer* **2010**;127:2106-18
18. Wischhusen J, Naumann U, Ohgaki H, Rastinejad F, Weller M. CP-31398, a novel p53-stabilizing agent, induces p53-dependent and p53-independent glioma cell death. *Oncogene* **2003**;22:8233-45

19. Christmann M, Kaina B. Nuclear translocation of mismatch repair proteins MSH2 and MSH6 as a response of cells to alkylating agents. *The Journal of biological chemistry* **2000**;275:36256-62
20. Christmann M, Tomicic MT, Aasland D, Berdelle N, Kaina B. Three prime exonuclease I (TREX1) is Fos/AP-1 regulated by genotoxic stress and protects against ultraviolet light and benzo(a)pyrene-induced DNA damage. *Nucleic acids research* **2010**;38:6418-32
21. Christmann M, Tomicic MT, Kaina B. Phosphorylation of mismatch repair proteins MSH2 and MSH6 affecting MutS{alpha} mismatch-binding activity. *Nucl Acids Res* **2002**;30:1959-66
22. Eich M, Roos WP, Nikolova T, Kaina B. Contribution of ATM and ATR to the resistance of glioblastoma and malignant melanoma cells to the methylating anticancer drug temozolomide. *Molecular cancer therapeutics* **2013**
23. Peng CY, Graves PR, Thoma RS, Wu Z, Shaw AS, Piwnica-Worms H. Mitotic and G2 checkpoint control: regulation of 14-3-3 protein binding by phosphorylation of Cdc25C on serine-216. *Science* **1997**;277:1501-5
24. Xiao Z, Chen Z, Gunasekera AH, Sowin TJ, Rosenberg SH, Fesik S, *et al.* Chk1 mediates S and G2 arrests through Cdc25A degradation in response to DNA-damaging agents. *The Journal of biological chemistry* **2003**;278:21767-73
25. Tomicic MT, Christmann M, Kaina B. Topotecan-triggered degradation of topoisomerase I is p53-dependent and impacts cell survival. *Cancer research* **2005**;65:8920-6
26. Fiorentino FP, Symonds CE, Macaluso M, Giordano A. Senescence and p130/Rb12: a new beginning to the end. *Cell research* **2009**;19:1044-51
27. Hartmann C, Kluwe L, Lucke M, Westphal M. The rate of homozygous CDKN2A/p16 deletions in glioma cell lines and in primary tumors. *International journal of oncology* **1999**;15:975-82
28. Iwasa H, Han J, Ishikawa F. Mitogen-activated protein kinase p38 defines the common senescence-signalling pathway. *Genes to cells : devoted to molecular & cellular mechanisms* **2003**;8:131-44
29. Coppe JP, Desprez PY, Krtolica A, Campisi J. The senescence-associated secretory phenotype: the dark side of tumor suppression. *Annual review of pathology* **2010**;5:99-118
30. Ren B, Cam H, Takahashi Y, Volkert T, Terragni J, Young RA, *et al.* E2F integrates cell cycle progression with DNA repair, replication, and G(2)/M checkpoints. *Genes & development* **2002**;16:245-56
31. Cam H, Balciunaite E, Blais A, Spektor A, Scarpulla RC, Young R, *et al.* A common set of gene regulatory networks links metabolism and growth inhibition. *Molecular cell* **2004**;16:399-411
32. Quiros S, Roos WP, Kaina B. Processing of O6-methylguanine into DNA double-strand breaks requires two rounds of replication whereas apoptosis is also induced in subsequent cell cycles. *Cell cycle* **2010**;9:168-78
33. Gire V, Dulic V. Senescence from G2 arrest, revisited. *Cell cycle* **2015**;14:297-304
34. Baus F, Gire V, Fisher D, Piette J, Dulic V. Permanent cell cycle exit in G2 phase after DNA damage in normal human fibroblasts. *The EMBO journal* **2003**;22:3992-4002
35. Charrier-Savournin FB, Chateau MT, Gire V, Sedivy J, Piette J, Dulic V. p21-Mediated nuclear retention of cyclin B1-Cdk1 in response to genotoxic stress. *Molecular biology of the cell* **2004**;15:3965-76
36. Krenning L, Feringa FM, Shaltiel IA, van den Berg J, Medema RH. Transient activation of p53 in G2 phase is sufficient to induce senescence. *Molecular cell* **2014**;55:59-72
37. Mullers E, Silva Cascales H, Jaiswal H, Saurin AT, Lindqvist A. Nuclear translocation of Cyclin B1 marks the restriction point for terminal cell cycle exit in G2 phase. *Cell cycle* **2014**;13:2733-43

38. Bunz F, Dutriaux A, Lengauer C, Waldman T, Zhou S, Brown JP, *et al.* Requirement for p53 and p21 to sustain G2 arrest after DNA damage. *Science* **1998**;282:1497-501
39. Lossaint G, Besnard E, Fisher D, Piette J, Dulic V. Chk1 is dispensable for G2 arrest in response to sustained DNA damage when the ATM/p53/p21 pathway is functional. *Oncogene* **2011**;30:4261-74
40. Thanasoula M, Escandell JM, Suwaki N, Tarsounas M. ATM/ATR checkpoint activation downregulates CDC25C to prevent mitotic entry with uncapped telomeres. *The EMBO journal* **2012**;31:3398-410
41. Wang D, Berglund A, Kenchappa RS, Forsyth PA, Mule JJ, Etame AB. BIRC3 is a novel driver of therapeutic resistance in Glioblastoma. *Scientific reports* **2016**;6:21710
42. Polager S, Kalma Y, Berkovich E, Ginsberg D. E2Fs up-regulate expression of genes involved in DNA replication, DNA repair and mitosis. *Oncogene* **2002**;21:437-46
43. Roos WP, Christmann M, Fraser ST, Kaina B. Mouse embryonic stem cells are hypersensitive to apoptosis triggered by the DNA damage O(6)-methylguanine due to high E2F1 regulated mismatch repair. *Cell death and differentiation* **2007**;14:1422-32
44. Mjelle R, Hegre SA, Aas PA, Slupphaug G, Drablos F, Saetrom P, *et al.* Cell cycle regulation of human DNA repair and chromatin remodeling genes. *DNA repair* **2015**;30:53-67
45. Silva AO, Dalsin E, Onzi GR, Filippi-Chiela EC, Lenz G. The regrowth kinetic of the surviving population is independent of acute and chronic responses to temozolomide in glioblastoma cell lines. *Experimental cell research* **2016**;348:177-83
46. Alvino E, Castiglia D, Caporali S, Pepponi R, Caporaso P, Lacal PM, *et al.* A single cycle of treatment with temozolomide, alone or combined with O(6)-benzylguanine, induces strong chemoresistance in melanoma cell clones in vitro: role of O(6)-methylguanine-DNA methyltransferase and the mismatch repair system. *International journal of oncology* **2006**;29:785-97
47. Felsberg J, Thon N, Eigenbrod S, Hentschel B, Sabel MC, Westphal M, *et al.* Promoter methylation and expression of MGMT and the DNA mismatch repair genes MLH1, MSH2, MSH6 and PMS2 in paired primary and recurrent glioblastomas. *International journal of cancer Journal international du cancer* **2011**;129:659-70
48. Stark AM, Doukas A, Hugo HH, Hedderich J, Hattermann K, Maximilian Mehdorn H, *et al.* Expression of DNA mismatch repair proteins MLH1, MSH2, and MSH6 in recurrent glioblastoma. *Neurological research* **2015**;37:95-105
49. Dosch J, Christmann M, Kaina B. Mismatch G-T binding activity and MSH2 expression is quantitatively related to sensitivity of cells to methylating agents. *Carcinogenesis* **1998**;19:567-73
50. McFaline-Figueroa JL, Braun CJ, Stanciu M, Nagel ZD, Mazzucato P, Sangaraju D, *et al.* Minor Changes in Expression of the Mismatch Repair Protein MSH2 Exert a Major Impact on Glioblastoma Response to Temozolomide. *Cancer research* **2015**;75:3127-38
51. Filippi-Chiela EC, Thome MP, Bueno e Silva MM, Pelegrini AL, Ledur PF, Garicochea B, *et al.* Resveratrol abrogates the temozolomide-induced G2 arrest leading to mitotic catastrophe and reinforces the temozolomide-induced senescence in glioma cells. *BMC cancer* **2013**;13:147
52. Kirkland JL, Tchkonja T, Zhu Y, Niedernhofer LJ, Robbins PD. The Clinical Potential of Senolytic Drugs. *Journal of the American Geriatrics Society* **2017**;65:2297-301

Legends to figures

Fig. 1: (A-D) Senescence was measured microscopically by detection of β -Gal positive cells. (A) LN229 cells were treated with inhibitors against ATR (ATR_i), ATM (ATM_i), DNA-PKcs (DNA-PKcs_i) and MRN (MRN_i). One hour later cells were treated with 50 μ M TMZ for 72h. In addition, also MGMT re-transfected cells were treated with TMZ. (B) U87 and LN229 cells

were non-treated or treated with TMZ (25 or 50 μ M TMZ) or TMZ/IR (25 μ M / 2Gy) at 5 consecutive days; senescence was measured at day 8. U87 (C) and LN229 cells (D) were treated with 50 μ M TMZ for different time points (left graph) or with different TMZ concentrations for 120 and 144 h (right graph). (E-H) Cell death was measured by flow cytometry using Annexin V / PI staining (left graph) and cell cycle distribution using PI staining (right graph). U87 (E) and LN229 cells (G) were non-treated or treated with TMZ (25 or 50 μ M TMZ) or TMZ/IR (25 μ M/2Gy) at 5 consecutive days; measurement occurred at day 8. U87 (F) and LN229 cells (H) were treated with 50 μ M TMZ for 120 and 144h. (A-H) Experiments were repeated at least three times, mean values \pm SD are shown. (A) Differences between TMZ treatment and TMZ/inhibitor treatment were statistically analyzed using Student's t test (* p <0.05, ** p <0.01).

Fig. 2: (A) p53 phosphorylation at Ser¹⁵ and p21 expression was determined by immunoblotting 48 to 120h after TMZ (100 μ M) exposure in U87 (left panel) and LN229 (right panel) cells. con = untreated cells. β -Actin was used as internal loading control. (B) p53 phosphorylation at Ser¹⁵, as well as p53 and p21 expression was determined by immunoblotting 24 to 48h after TMZ (100 μ M) exposure in LN229, LN308, U87 and U138 cells. (C) p21 mRNA expression was measured by RT-qPCR, 24 to 72h after TMZ (100 μ M) exposure in LN229, LN308, U87 and U138 cells. (D) Concentration dependent induction of senescence was measured by detection of β -Gal positive cells 120 and 144h after TMZ exposure in U138 and LN308 cells. (E) Cell cycle distribution was measured using PI staining and flow cytometry, 120h after TMZ exposure in U138 and LN308 cells. (F/G) LN229 and U87 cells were transfected with non-silencing siRNA (ns-si) and p21 specific siRNA (p21-si). 16 h later cells were treated with 100 μ M TMZ. 120h later, senescence was measured by detection of β -Gal positive cells (F) and cell cycle distribution was measured using PI staining and flow cytometry (G). (A-G) Experiments were repeated at least three times, mean values \pm SD are shown. (F) Differences between TMZ/ns-si treatment and TMZ/p21-si treatment were statistically analyzed using Student's t test (** p <0.001).

Fig. 3: (A) Phosphorylation of CHK1 and CHK2, as well as expression of CDC25a and CDC25c was determined by immunoblotting 48 to 96h after TMZ (100 μ M) exposure in U87 (left panel) and LN229 (right panel) cells. (B-D) U87 and LN229 cells were treated with inhibitors against CHK1 (UCN-01 = CHK1_i), CHK2 (CHK2_i) and p21 (UC2288 = p21_i) and one hour later with 100 μ M TMZ. (B) Expression of CDC25c was determined by immunoblotting 72h upon TMZ exposure. (C) Cell cycle distribution was measured using PI staining and flow cytometry 72h after TMZ exposure. Experiments were repeated at least three times, mean values \pm SD are shown. (D) Induction of senescence was measured by

FACS based detection of C₁₂FDG positive cells 120h after TMZ exposure. Differences between TMZ treatment and TMZ/inhibitor treatment were statistically analyzed using Student's t test (*p<0.05, ****p<0.0001). (E) LN229 cells were treated with inhibitors against ATR (VE-821 = ATR_i), ATM (KU60019 = ATM_i), DNA-PKcs (KU0060648 = DNA-PKcs_i) and MRN (Mirin = MRN_i). One hour later cells were treated with 50 μM TMZ for 72h and cell cycle distribution was measured. In addition, also MGMT re-transfected cells were treated with TMZ. (C-E) Experiments were repeated at least three times, mean values ± SD are shown.

Fig. 4: (A) LN229 and U87 cells were treated with 100 μM TMZ for different time points (left graph) or cells were non-treated or treated with TMZ (25 or 50 μM TMZ) or TMZ/IR (25 μM/2Gy) at 5 consecutive days; protein isolation occurred at day 8 (right panel). Expression of IκB was determined by immunoblotting. (B) U87 and LN229 cells were treated with 100 μM TMZ for different time points. Secretion of IL6 and IL8 was measured by ELISA. (C/D) U87 and LN229 cells were treated with 50 μM TMZ and 48 later with the NF-κB inhibitor III. (C) Senescence was measured 144h upon TMZ exposure via β-Gal staining and flow cytometry-based acquisition of C₁₂FDG positive cells. (D) Cell death was measured using Annexin V / PI staining and flow cytometry. (B-D) Experiments were repeated at least three times, mean values ± SD are shown. (C-D) Differences between TMZ treatment and TMZ/inhibitor treatment were statistically analyzed using Student's t test (*p<0.05, **p<0.01, ***p<0.001). E) U87 and LN229 cells treated with 100 μM TMZ in the presence or absence of NF-κB inhibitor III. 72h later, expression of *c-IAP2*, *XIAP*, *BCL-X_L* and *Survivin* mRNA was measured by RT qPCR.

Fig. 5: (A) Time-dependent expression of *EXO1*, *MSH2*, *MSH6*, *RAD51* and *DDB2* was determined by RT qPCR after TMZ (100 μM) exposure in U87 and LN229 cells. Expression was normalized to *gapdh* and *β-actin*; the untreated control was set to one. (B) Time-dependent expression of EXO1, MSH2, MSH6, RAD51 protein was determined after TMZ (100 μM) exposure by immunoblotting in U87 and LN229 cells. β-Actin was used as internal loading control. (C) U87 and LN229 cells were non-treated or treated with TMZ (25 or 50 μM TMZ) or TMZ/IR (25 μM/2Gy) at 5 consecutive days; protein isolation occurred at day 8. Expression of EXO1, MSH2, MSH6, RAD51 was determined by immunoblotting. β-Actin was used as internal loading control. (D/E) U87 and LN229 cells were treated with 100 μM TMZ for 72 and 96h. (D) MSH2/MSH6 binding activity was analyzed by EMSA. (E) HR activity was analyzed using the PCR-based HR Assay Kit from Norgen Biotec Corp. ID 35600.

Fig. 6: (A) LN229 and U87 cells were treated with 100 μM TMZ for 72 and 96h. (B) LN229 cells and U87 cells were non-treated or treated with TMZ (25 or 50 μM TMZ) or TMZ/IR (25

μM / 2Gy) at 5 consecutive days; protein isolation occurred at day 8 (right panel). (A/B) Whole cell extracts were prepared and E2F1 was immunoprecipitated (IP) using specific antibody against E2F1. 50% of the immunoprecipitated proteins were separated by SDS page and E2F1 was detected by immunodetection. 50% of the immunoprecipitated proteins were separated by SDS page and DP1 was detected by immunodetection. (C/D) ChIP analysis was performed in U87 and LN229 cells 72h after exposure to 100 μM TMZ. Protein-DNA complexes were immuno-precipitated with anti-E2F1 (C) or anti-DP1 (D) antibody and real time PCR was performed using primers flanking the E2F1-responsive element within the *EXO1*, *MSH2*, *MSH6* and *RAD51* promoter. (E) U87 and LN229 cells were transfected with non-silencing siRNA (ns-si) and p21 specific siRNA (p21si). 24 h later cells were treated with 100 μM TMZ and 72h later the expression of *EXO1*, *MSH2*, *MSH6* and *RAD51* mRNA was measured by RT qPCR.

Fig. 7: LN229 (A) and U87 (B) cells were non-treated (con) or treated with 100 μM TMZ for 120h (TMZ). In parallel cells were treated with 100 μM TMZ for 120h and C_{12}FDG positive cells were separated by FACS (sen). Senescence was verified *via* β -Gal staining (left panel) and cell cycle distribution was measured using PI staining (middle panel). Whole cell extracts were prepared and *EXO1*, *MSH2*, *MSH6* and *RAD51* were detected by immunodetection (right panel); β -Actin was used as internal loading control. (C) U87 cells were injected into immunodeficient (Balb/c nu/nu) mice. Upon tumour formation the mice were either mock-treated or treated with TMZ (200 mg/kg body weight in DMSO/NaCl i.p.). 96h later, mice were sacrificed and the tumours isolated. For analysis the left and right tumour were combined and protein expression of various proteins was determined by immunoblotting. (D) Model summarizing TMZ-induced senescence. Upon TMZ exposure, the initial damage O^6MeG is processed into replication stressing lesions via futile mismatch repair (MMR) cycles, leading to the activation of the DDR. ATR activates CHK1, which targets CDC25c for degradation, leading to abrogated CDK1 activation and G2/M arrest. In parallel, the DDR activates p53, leading to the expression of p21, which causes nuclear retention of the inactive CDK1/CyclinB1 complex, thereby prolonging the G2/M arrest. We suppose that other, unknown functions of p21 are additionally required for the induction and maintenance of senescence. Furthermore, degradation of I κ B and, thereby, activation of NF- κ B is required for TMZ-induced senescence through induction of the SASP, which maintains senescence and prevents from apoptosis.

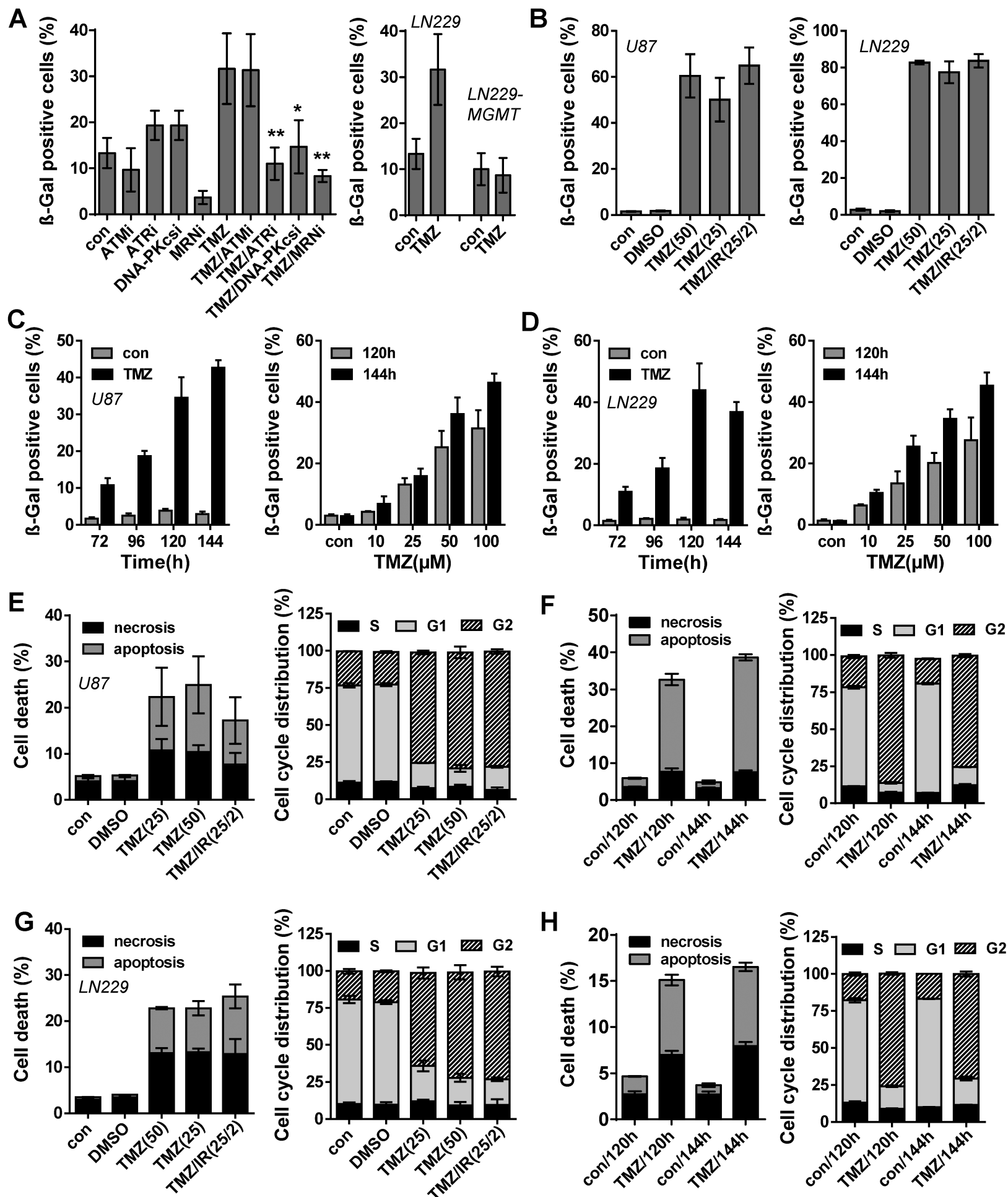


Fig. 1

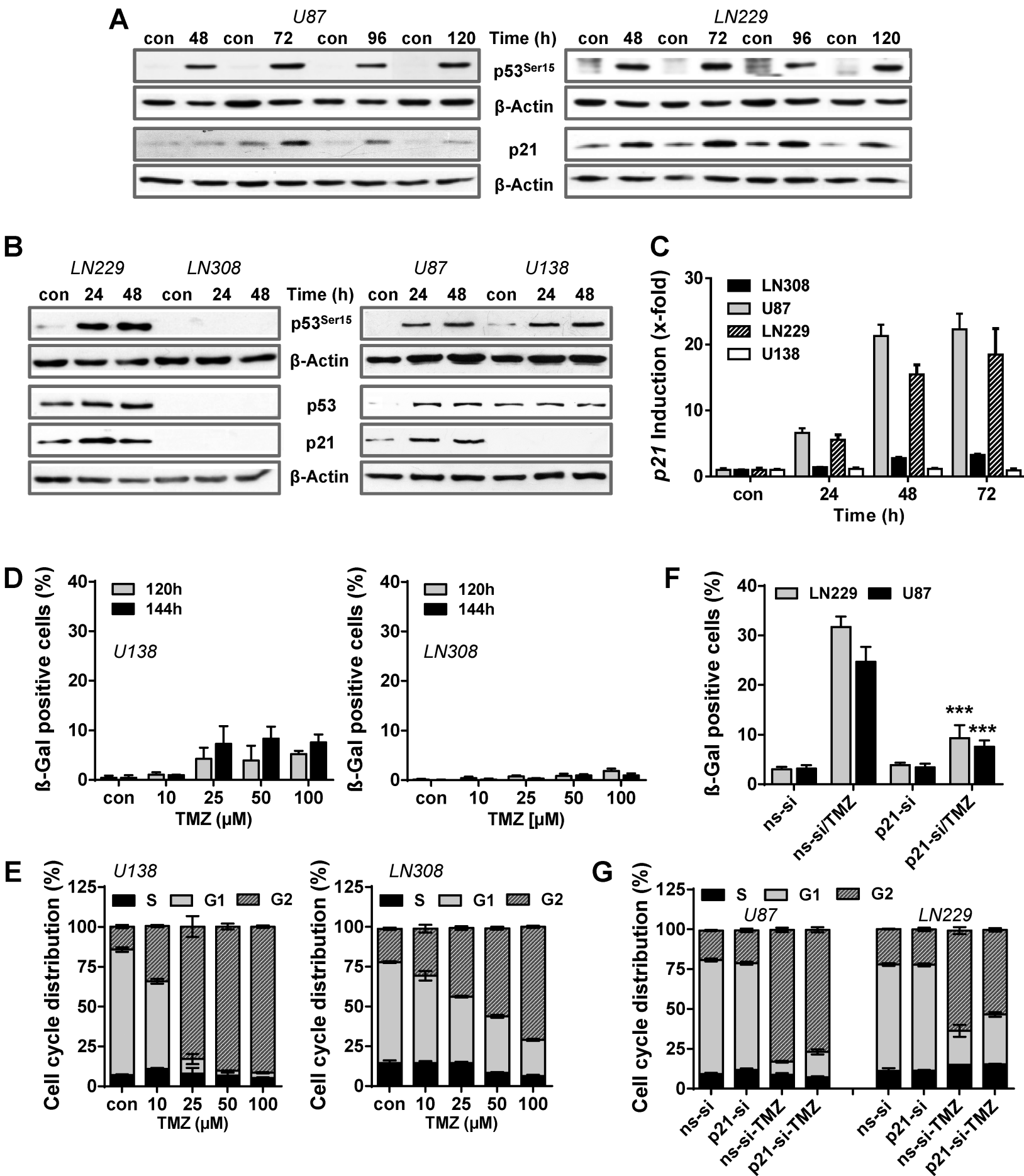
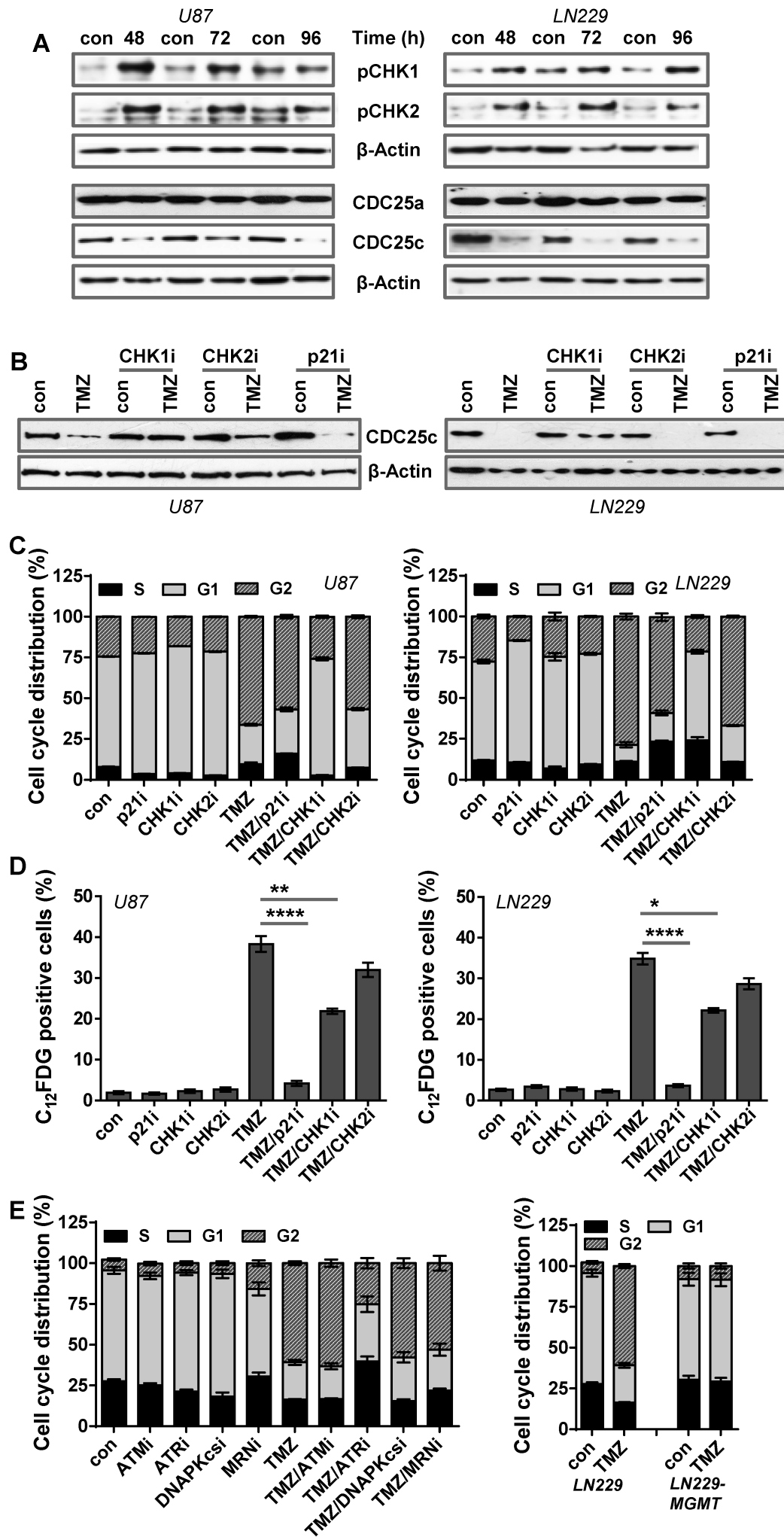


Fig.2



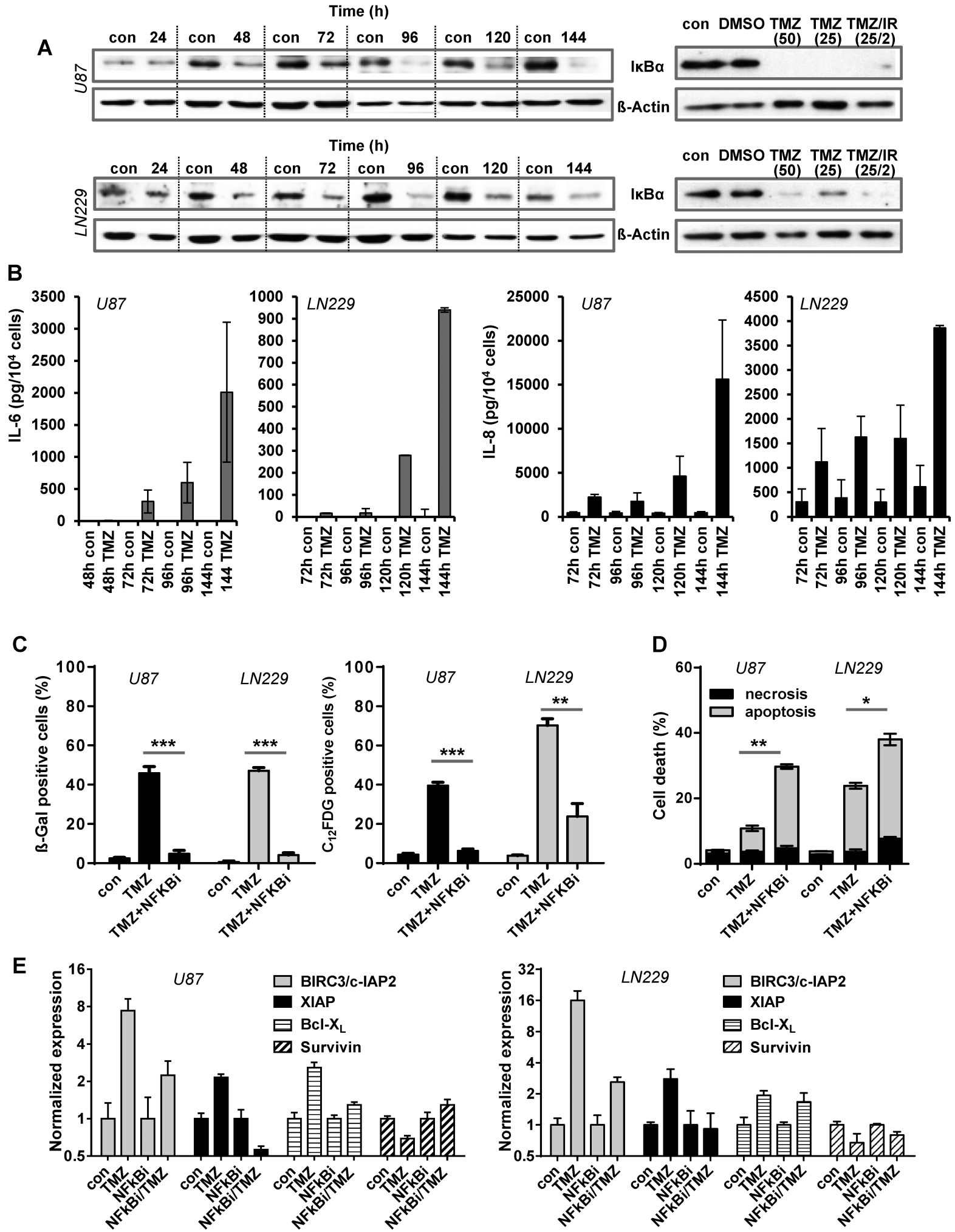


Fig.4

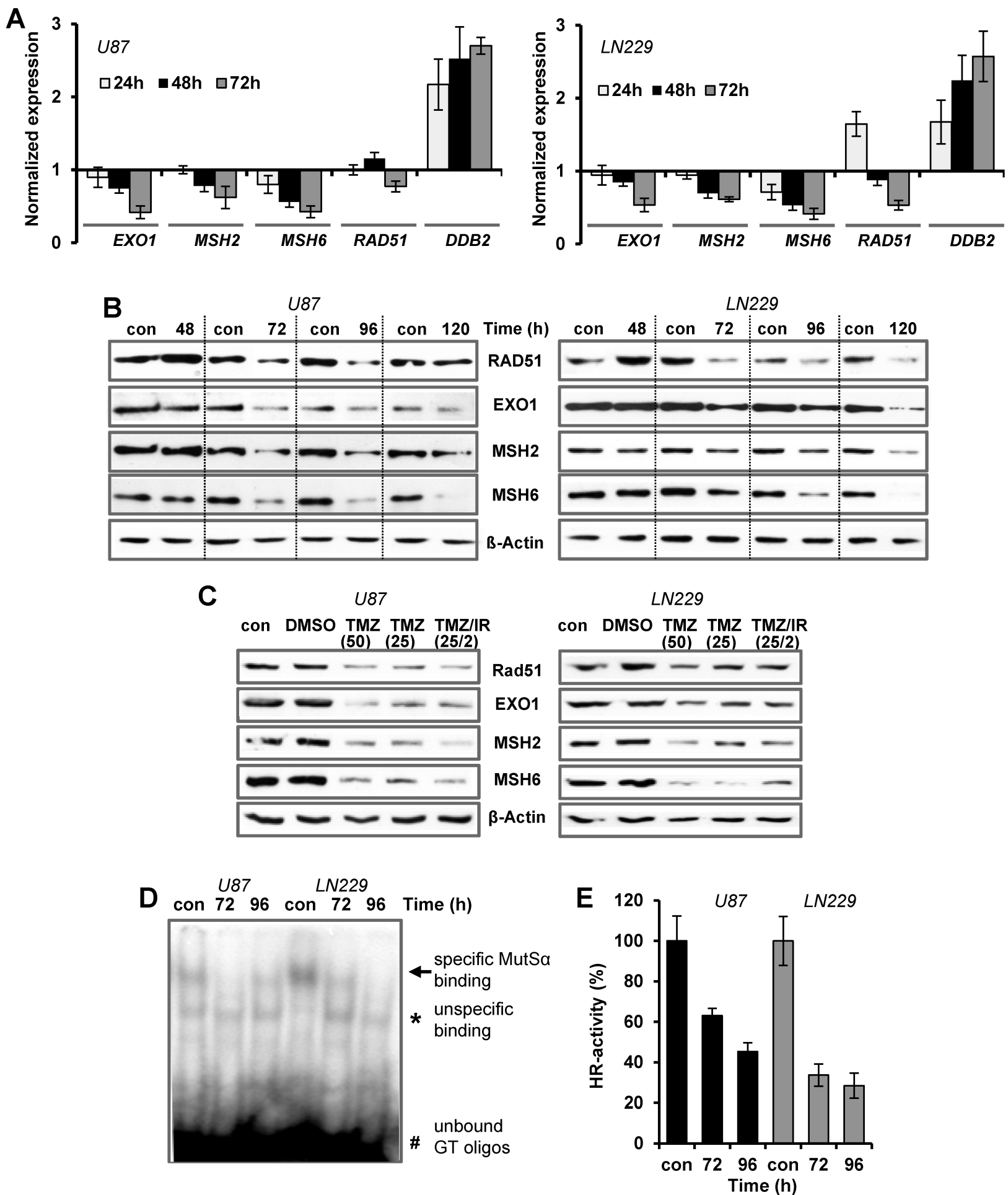


Fig.5

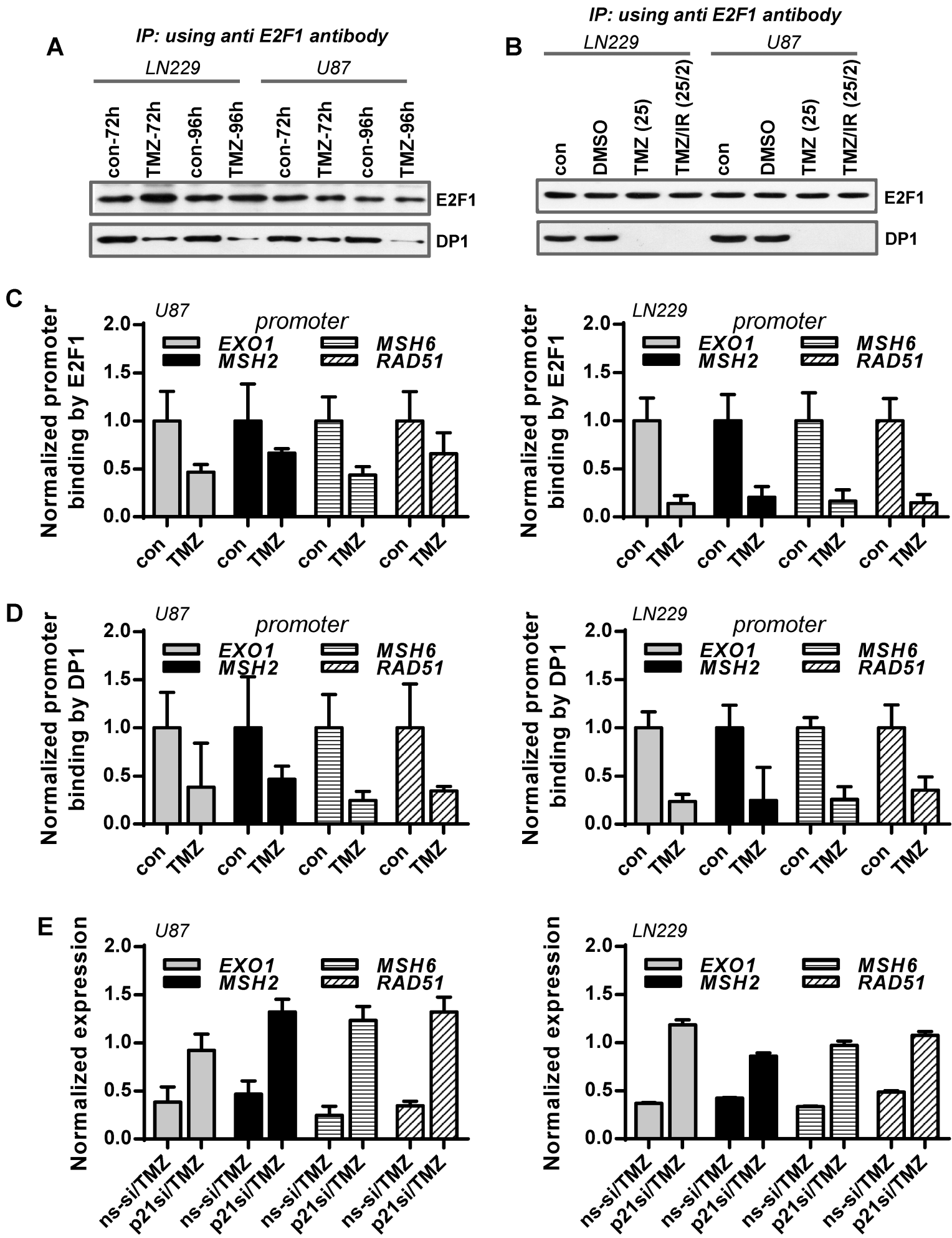
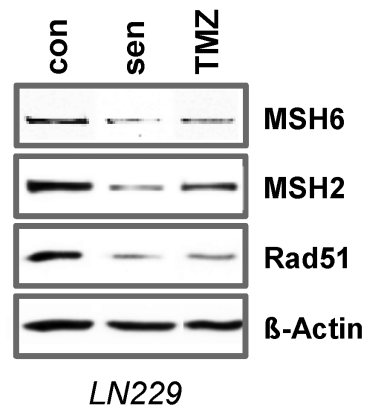
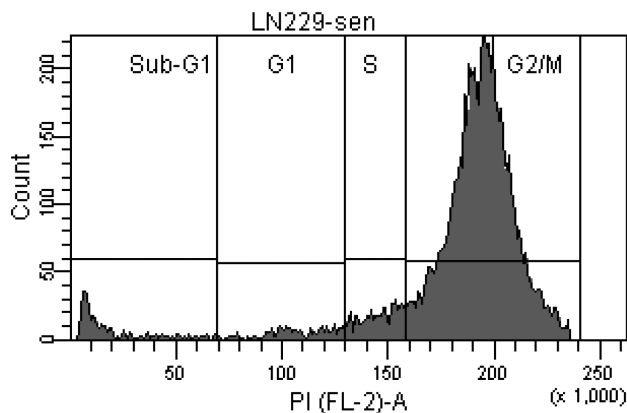
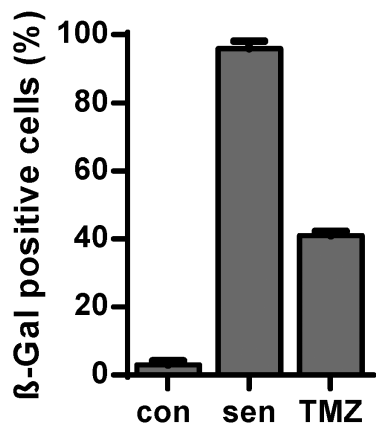
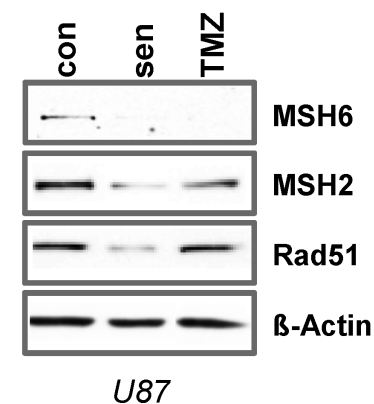
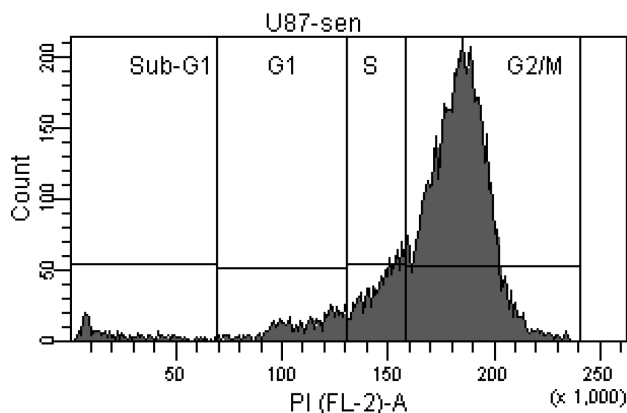
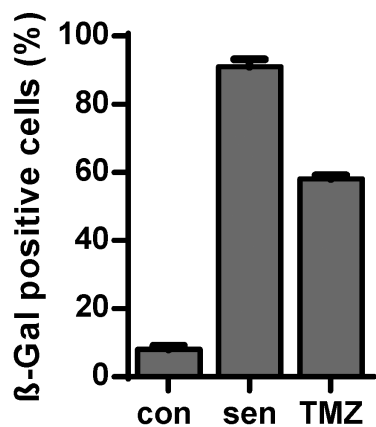
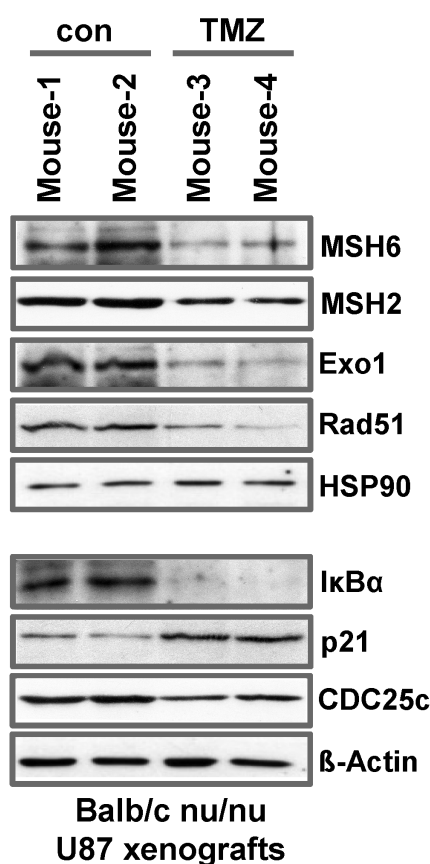
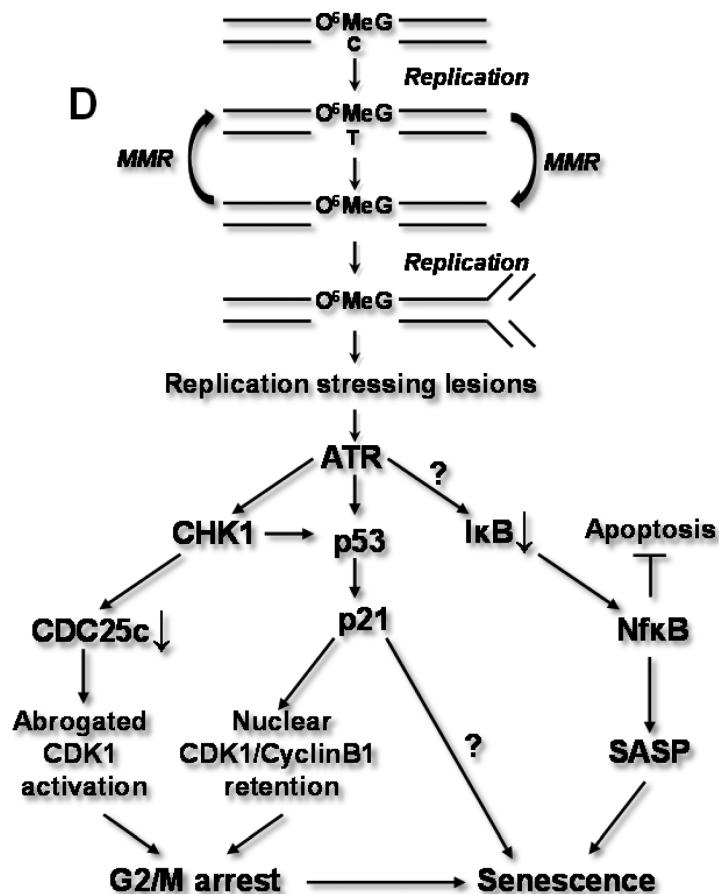


Fig.6

A**B****C****D**

Cancer Research

The Journal of Cancer Research (1916–1930) | The American Journal of Cancer (1931–1940)

Temozolomide induces senescence and repression of DNA repair pathways in glioblastoma cells via activation of ATR-CHK1, p21, and NF- κ B

Dorthe Aasland, Laura Göttinger, Laura Hauck, et al.

Cancer Res Published OnlineFirst October 25, 2018.

Updated version	Access the most recent version of this article at: doi: 10.1158/0008-5472.CAN-18-1733
Supplementary Material	Access the most recent supplemental material at: http://cancerres.aacrjournals.org/content/suppl/2018/10/25/0008-5472.CAN-18-1733.DC1
Author Manuscript	Author manuscripts have been peer reviewed and accepted for publication but have not yet been edited.

E-mail alerts	Sign up to receive free email-alerts related to this article or journal.
Reprints and Subscriptions	To order reprints of this article or to subscribe to the journal, contact the AACR Publications Department at pubs@aacr.org .
Permissions	To request permission to re-use all or part of this article, use this link http://cancerres.aacrjournals.org/content/early/2018/10/25/0008-5472.CAN-18-1733 . Click on "Request Permissions" which will take you to the Copyright Clearance Center's (CCC) Rightslink site.